

## **Durability Simulation of Elastomeric Materials Using Finite Element Method (FEM)**

**C. W. Chieh, Aidy Ali\*, Asmawi Sanuddin and Reza Afshar**

*Department of Mechanical and Manufacturing Engineering,  
Faculty of Engineering, Universiti Putra Malaysia,  
43400 UPM, Serdang, Selangor, Malaysia*

*\*E-mail: aidy@eng.upm.edu.my*

### **ABSTRACT**

The paper presents a simulation work conducted on the elastomer subjected to cyclic loads. A 3D finite element model of elastomer specimen, in accordance to ASTM D412, was developed using CATIA and ANSYS commercial finite element (FEM) packages. Fatigue life predicted from the simulation was compared with well-documented published data and it showed an acceptable agreement. Meanwhile, the simulated strain-life results are slightly lower than the experimental data. Several factors which potentially influenced the variations of the results were noted. Finally, some recommendations are offered at the end of this study to further improve the simulation.

**Keywords:** Elastomer, FEM, strain controlled loading, CATIA, ANSYS

### **INTRODUCTION**

Synthetic polymers such as elastomers consist of a large family of amorphous polymers with a low elastic modulus; they can be stretched to at least twice their original length and return quickly to the original length when stress is released (Philip, 2006). These polymeric materials are widely used in applications where low stiffness and a high elastic strain are required. They are commonly used in many demanding applications, from tyres and seals to gloves and medical devices. The failure of rubber products in these demanding applications would cause disaster. In many of these applications, the component experiences cyclic loading and failure is due to a fatigue.

Fatigue is a phenomenon of failure of material under cyclic or long-term stress at stress levels well below their ultimate stress and it is the result of the progressive growth of cracks through the material (Hall, 1979). Generally, elastomers can fail due to either thermal fatigue or mechanical fatigue. The failure is caused by factors such as load frequency, stress level, temperature, and the geometry of the component. The observation carried out showed that the fatigue process involved the following states: (1) crack nucleation, (2) short crack growth, (3) long crack growth, and (4) final fracture. Fatigue starts with crack nucleation and when cyclic loading continues, the crack tends to grow along the plane of maximum shear stress through grain boundary (Lee *et al.*, 2005).

In fact, cracks cannot be avoided in many structural applications. The location and size of these cracks will influence the fatigue life of any structure. For elastomers, their fatigue life is affected by some parameters such as the size and distribution of the initial defects, stress concentrations within the sample geometry or it can be caused by processing, molecular distribution, as well as degree of cross-linking in the microstructure, and environmental influences like test temperature and exposure to aggressive chemicals (for example, UV light, oils, ozone) (Hainsworth, 2007). In order to predict the fatigue life of any component, a fatigue analysis is needed to provide a sound basis of lifespan of the designed components.

---

Received: 23 November 2009

Accepted: 5 March 2010

\*Corresponding Author

According to Andriyana and Verron, (2007) two approaches are generally adopted to define end of life (Mars and Fatemi, 2002); the crack nucleation approach and the crack growth approach. The former defines fatigue life as the number of cycles required to create a crack of a given size. This approach, which follows the work of Wohler (1867), was applied to rubber by Cadwell *et al.* (1940), considering the fact that fatigue life of rubbers can be determined from the history of strain and stress at each material point of the body. Meanwhile, the second approach defines fatigue life as the number of cycles required by the pre-existing crack to grow to the point of failure. The idea of considering pre-existing cracks or flaws was introduced by Inglis (1913) and Griffith (1920), but it was Rivlin and Thomas (1953) who first applied it to rubber (Andriyana and Verron, 2007; Fetemi and Mars, 2002).

Fatigue life prediction under loadings is crucial in structure design. Therefore an appropriate fatigue life criterion is necessary to prevent their fracture in service (Saintier *et al.*, 2006). In the previous studies, fatigue life prediction in metallic materials has been largely investigated over the past decades and it is still of major concern (Papadopoulos *et al.*, 1997; Doblare, 2002; Liu *et al.*, 2005; Makkonen, 2009). However, fatigue life prediction in rubbers has limited investigation as compared to metallic materials, despite the growing use of rubbers in a wide range of industrial applications (Saintier *et al.*, 2006). Therefore, the objectives of this work are: (1) to develop a finite element model (FEM) of natural rubber under cyclic loadings, and (2) to predict the life of elastomer specimens under cyclic loads through the developed FEM model.

#### FINITE ELEMENT METHOD (FEM) AND ELASTOMERIC FATIGUE MODELLING

The Finite Element Method (FEM) is a numerical procedure that can be used to obtain solutions to a large class engineering problems involving stress analysis, heat transfer, vibration, deflection, buckling behaviour, and many other phenomena (Osman, 2004; Marcus *et al.*, n.d.; Lira *et al.*, 2002). This method can be used to analyze either small or large-scale deflection under loading or applied displacement. The simulation is required because of the astronomical number of calculations needed to analyze a large structure. The finite element analysis is a way to deal with structures which are more complex than can be dealt with analytical solution using classical theories (Chan *et al.*, 2006; Hertzberg, 1996). The key idea of the finite element method is to discretize the solution domain into a number of simpler domains called elements. An approximate solution is assumed over an element in terms of solution at selected points called nodes (Bhatti, 2005).

There are several forms of strain energy potentials available to model the incompressible and isotropic elastomers. They are the Mooney-Rivlin model (Green and Addkins, 1970), the Ogden (1984) model, the Yeoh (1993) model, the Arruda and Boyce (1993) model, the Van der Waals model (Kilian *et al.*, 1996), the neo-Hookean model, the polynomial model, and the reduced polynomial model (Weber and Anand, 1990). By comparing these options after performing hyperelastic material curve fitting, the Ogden was chosen since it provides the best approximation to a solution at larger strain levels. In the Ogden model, the strain energy potential is represented as:

$$U = \sum_{i=1}^N \frac{2\mu_i}{\alpha_i^2} (\bar{\lambda}_1^{\alpha_i} + \bar{\lambda}_2^{\alpha_i} + \bar{\lambda}_3^{\alpha_i} - 3) + \sum_{i=1}^N \frac{1}{D_i} (J - 1)^{2i} \quad (1)$$

Where,

- $\bar{\lambda}_i = J^{-\frac{1}{3}} \lambda_i =$  deviatoric principal stretches
- $\lambda_i =$  principal stretches
- $J =$  Jacobian determinant of the deformation gradient
- $N =$  number of terms in the series
- $\mu_p, \alpha_p, D_i =$  temperature dependent material parameters

By assuming the material is incompressible, therefore, in the uniaxial stress state, the principal stretches  $\lambda_i$  are represented by:

$$\lambda_1 = \lambda_u, \quad \lambda_2 = \lambda_3 = \frac{1}{\sqrt{\lambda_u}} \quad (2)$$

The nominal strain in the loading direction is given by:

$$\varepsilon_U = \lambda_U - 1 \quad (3)$$

Where,

$$\begin{aligned} \lambda_u &= \text{stretch in the loading direction} \\ \varepsilon_u &= \text{nominal strain in the loading direction} \end{aligned}$$

The uniaxial nominal normal stress,  $T_U$ , is determined by considering the principle of virtual work (Ogden, 1984) in the form of:

$$T_U = \frac{\partial U}{\partial \lambda_U} \quad (4)$$

By letting  $N=1$  and substituting equation (2) into equation (1), the strain energy potential for the uniaxial stress state is represented by:

$$\begin{aligned} U &= \frac{2\mu_1}{\alpha_1^2} (\lambda_U^{\alpha_1} + 2\lambda_U^{-\alpha_1/2} - 3) \\ &= \frac{2\mu_1}{\alpha_1^2} [(1 + \varepsilon_U)^{\alpha_1} + 2(1 + \varepsilon_U)^{-\alpha_1/2} - 3] \end{aligned} \quad (5)$$

From equations (4) and (5), the nominal stress and strain relation under uniaxial tension is expressed as:

$$\begin{aligned} T &= \frac{2\mu_1}{\alpha_1} (\lambda_U^{\alpha_1-1} - \lambda_U^{-(\alpha_1/2+1)}) \\ &= \frac{2\mu_1}{\alpha_1} [(1 + \varepsilon_U)^{\alpha_1-1} - (1 + \varepsilon_U)^{-(\alpha_1/2+1)}] \end{aligned} \quad (6)$$

In order to define the hyperelastic material behaviour, such as constitutive relation, experimental test data are required to determine material parameters in the strain energy potential (Wang *et al.*, 2002; Kim *et al.*, 2004). Therefore, material parameters,  $\alpha_1$  and  $\mu_1$ , can be determined by fitting the experimental nominal stress-strain curve into Equation (6) (Wang *et al.*, 2002).

## SIMULATION WORK

In this study, an elastomer material under uniaxial zero based cyclic loading of strain ratio,  $r = \text{minimum strain}/\text{maximum strain} = 0$  with strain controlled, was analyzed. A 0.1 Hz frequency of triangular strain wave was used. The strain amplitude was measured by dividing the cross-head displacement and the gauge length of the specimen. The geometric modelling and simulation are respectively performed by CATIA and ANSYS Multiphysics. For the experimental work, the material used is a carbon-filled natural rubber with 65 parts of carbon black mixed with 100 parts of natural rubber having an international rubber hardness degree (IRHD) of 72 (Wang *et al.*, 2002).

### *Geometry Modelling in CATIA*

In simulation, all dimensions in CATIA were measured in mm. The nominal dimensions of the ASTM D412 specimens are shown in *Fig. 1*. The geometry of model shown in the figure is symmetry at horizontal and vertical. Since then, a quarter part of the specimen was drawn on YZ plane and this was followed by creating the full image. The 3D drawing was obtained by extruding the full image to 1.9 mm in x direction and perpendicular to YZ plane.

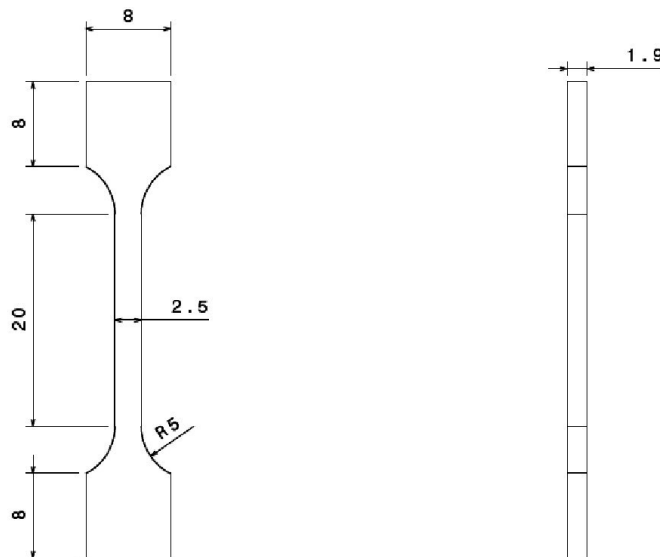


*Fig. 1: Dimensions of ASTM D412 specimen (all dimensions in mm)  
(Hertzberg, 1996)*

### *Mesh Generation*

The element used on the ASTM D412 specimen was SOLID187 which is defined by 10 nodes and there are three degrees of freedom at each node. There are translations in x, y, and z directions. The mesh of the specimens was completed by clicking on the volume and selecting all parts; the display of the mesh generation is shown in *Fig. 2(a)*. The mesh relevance value was set to be 100, as shown in *Fig. 2(b)*. Since the model would undergo large deformation, the “Aggressive Mechanical” in “Shape Checking” was therefore selected.

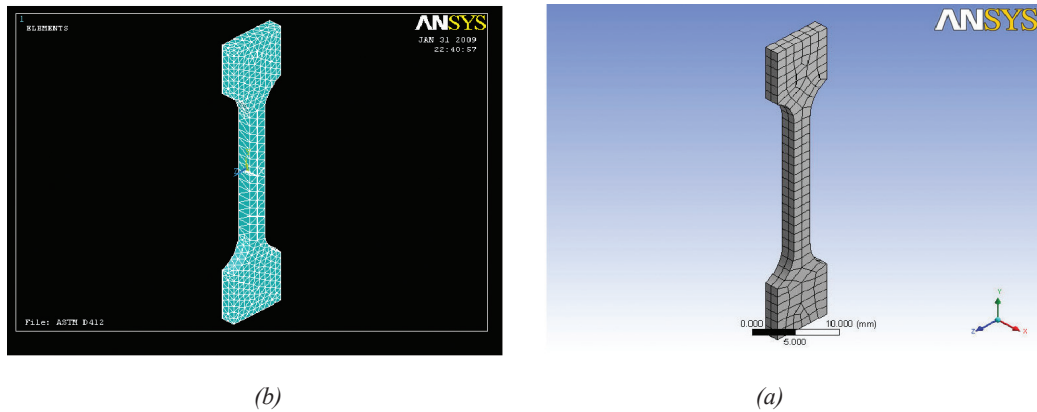


Fig. 2: Mesh generation in (a) ANSYS and (b) ANSYS Workbench

### Import Data and Material Curve Fitting

The stress-strain data and stress-life data from the experimental results were imported into ANSYS Multiphysics, while the hyperelastic and material curve fitting was performed as shown in Fig. 3. The Ogden model was chosen among other options because it provides the best approximation to a solution at larger strain levels up to 700% (the maximum strain level in the extracted experimental data is up to 385%). From the Ogden Order 1 model, yield  $\alpha_1=2.8373$  and  $\mu_1=1.6354$ MPa. In order to set the constraint, the displacement values, ranging from 140 mm - 480 mm (70%-240%), were applied in Area 3. For each value of the strain, the fatigue calculation was performed. After that, the displacement constrain was applied in Area 1 in y-direction and Area 2 in x-direction. Fig. 4 shows Areas 1, 2, 3, and 4 of the model, respectively. In the experiment, however, both ends were clamped (Area 4) and the upper end of the specimen was displaced in positive y-direction. At the same time, the reduction of thickness also occurred. Generally, the boundary condition applied in Area 2 for both the experiment and simulation are the same.

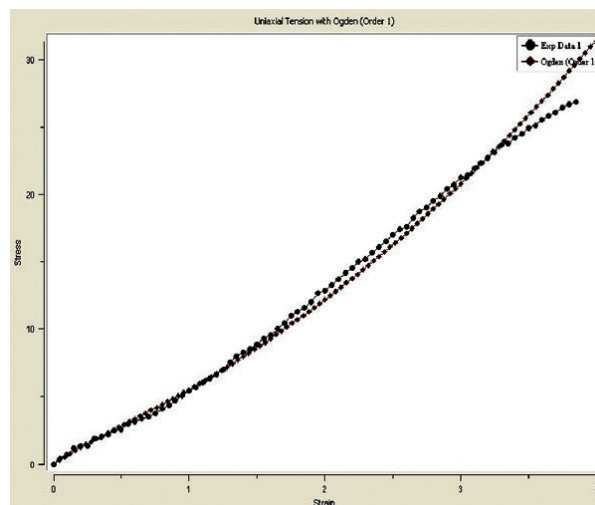


Fig. 3: Hyperelastic material curve fitting

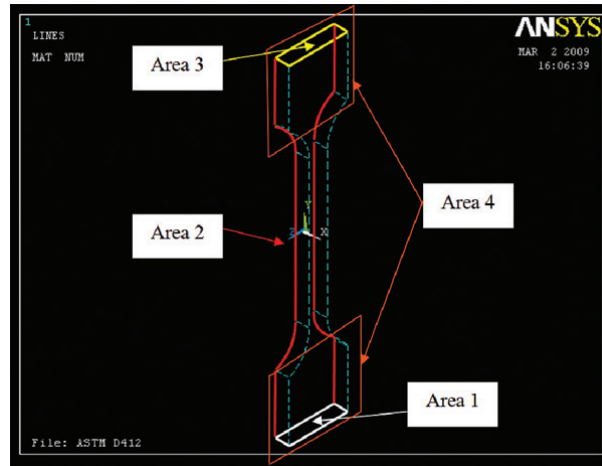


Fig. 4: Areas 1, 2, 3 and 4 of the model

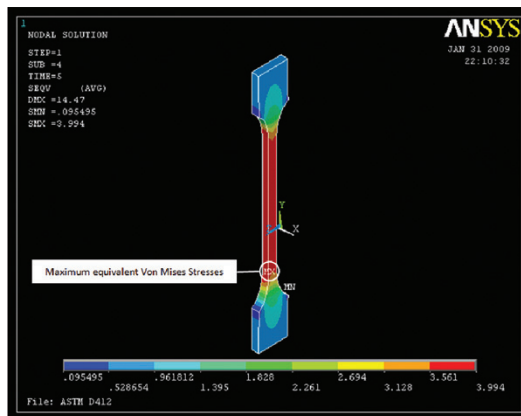


Fig. 5: Maximum SEQV at node 2544

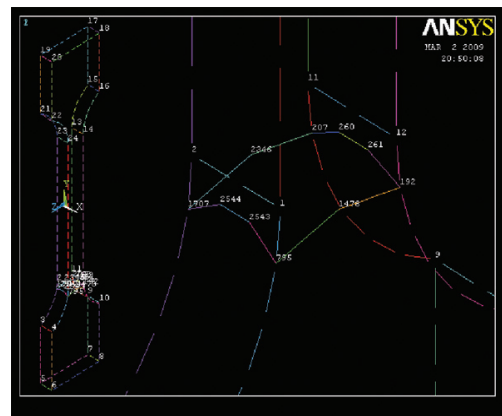


Fig. 6: Location of the 10 nodes

*Post-processing*

In this section, the nodal solution result was chosen to present the stress results. From the nodal solution, the equivalent Von Mises (SEQV) stresses were used to determine the failure location of the model. Fig. 5 shows that the maximum SEQV occurred at the same location (node 2544 in ANSYS) for all the values of strain.

In the ANSYS simulation environment, the fatigue life of the model was measured at the shortest life of 10 critical nodes. These nodes are the node of 192, 207, 260, 261, 795, 1478, 1707, 2346, 2543, and 2544 and their positions are shown in Fig. 6. On the other hand, the fatigue life which was calculated in the ANSYS Workbench simulation environment is the fatigue life of the whole model rather than of a particular node.

## Durability Simulation of Elastomeric Materials Using Finite Element Method (FEM)

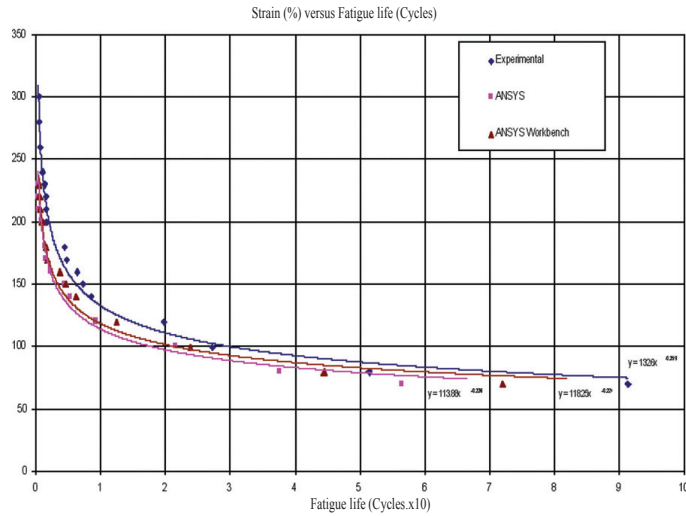


Fig. 7: A comparison between three types of predicted strain-life curve

### RESULTS AND DISCUSSION

The fatigue life cycles of the model predicted by ANSYS were obtained and these results were compared with well-documented experimental data for validation. A table of comparison is tabulated in Table 1. In order to compare the simulations and the experimental results, the fatigue life of the model at different strain percentages (i.e. between 70%-240%) was calculated with the software. The negative sign in the percentage difference indicates that the simulation fatigue life is smaller than the experiment fatigue life.

For the ease of comparison, all the fatigue data were plotted in a graph, as shown in Fig. 7. From the graph, both the predicted fatigue life cycles of the model are slightly lower than the experimental fatigue life. This state occurs because the experimental fatigue life cycles were taken when the tested specimen was broken into two pieces; however, the fatigue life cycles taken by the ANSYS and ANSYS Workbench the cycles when the failure of a particular node. This is considered as the life of a complete fracture versus the life of an initiated crack.

TABLE 1  
A comparison between the simulation and experimental results

Strain (mm)	Strain percentage (%)	Experimental fatigue life (Cycles)	ANSYS predicted fatigue life (Cycles)	Differences in the percentages between ANSYS and experiment (%)	ANSYS Workbench predicted fatigue life (Cycles)	Differences in the percentage between ANSYS Workbench and experiment (%)
14	70	91201	56430	-38	71846	-21
16	80	51310	37570	-27	44365	-14
20	100	27219	21580	-21	23777	-13
24	120	19735	9261	-53	12336	-37
28	140	8438	5328	-37	6188	-27
30	150	7250	4402	-39	4602	-37
32	160	6310	2389	-62	3635	-42
34	170	4671	1580	-66	1720	-63
36	180	4332	1451	-67	1535	-65
40	200	1600	960	-40	898	-44
42	210	1568	552	-65	592	-62
44	220	1468	466	-68	526	-64
46	230	1260	381	-70	424	-66
48	240	1000	-	-	-	-
52	260	602	-	-	-	-
56	280	511	-	-	-	-
60	300	381	-	-	-	-

### CONCLUSIONS

A three-dimensional finite element analysis was used to examine the fatigue life cycles of the ASTM D412 specimens and comparisons were made to the well-documented experimental data. These comparisons show similarity in terms of the shape of the plotted strain-life curves and a slight difference in terms of the fatigue life cycles of the specimen. Meanwhile, a finite element model has successfully been developed and it can be applied for the prediction of other materials, load, and size of geometry under cyclic loading. In short, FEM gives a good control of the experimental techniques, confirming, complementing and refining the specimen design before commencing any experiment tests.

### ACKNOWLEDGEMENT

The authors would like to thank the Ministry of Higher Education, Malaysia, for the financial support granted.



## REFERENCES

- Andriyana, A. and Verron, E. (2007). Prediction of fatigue life improvement in natural rubber using configurational stress. *The International Journal of Solids and Structures*, 44, 2079-2092.
- Andriyana, A. and Verron, E. (2005). Effect of the hysteretic response of elastomers on the fatigue life. In P.E. Austrell and L. Kari (Eds.), *Constitutive models for rubber IV* (pp. 31-36). A.A. Balkema Publishers.
- Arruda, E.M. and Boyce, M.C. (1993). Three-dimensional constitutive model for the large stretch behavior of rubber elastic materials. *Journal of the Mechanics and Physics of Solids*, 41(2), 389.
- Bea, J.A. and Doblare, M. (2002). Enhanced B-PFEM Model for fatigue life prediction of metals during crack propagation. *Computational Material Sciences*, 25, 14-33.
- Bhatti, M.A. (2005). *Fundamental Finite Element Analysis and Applications: With Mathematica and Matlab Computations*. John Wiley & Sons, Inc.
- Cadwell, M., Merrill, R., Sloman, C. and Yost, F. (1940). Dynamic fatigue life of rubber. *Industrial and Engineering Chemistry Research*, 12(1), 19-23.
- Chan, O.B., Elwi, A.E. and Gilbert, G.Y. (2006). Simulation of crack propagation in steel plate with strain softening model. Structural Engineering Report No. 266.
- Fatemi, A. and Mars, W.V.A. (2002). Literature survey on fatigue analysis approaches for rubber. *International Journal of Fatigue*, 24, 949-961.
- Green, A.E. and Adkins, J.E. (1970). *Large Elastic Deformations*. Oxford: Clarendon Press.
- Griffith, A. (1920). The phenomena of rupture and flow in solids. *Philosophical Transactions of the Royal Society London A*, 221, 163-198.
- Hainsworth, S.V. (2007). An environmental scanning electron microscopy investigation of fatigue crack initiation and propagation in elastomers. *Polymer Testing*, 26, 60-70.
- Hall, R.O. (1979). Rubber as an engineering material. *International Journal of Material Engineering Applications*, 1, 295-302.
- Hertzberg, R. (1996). *Deformation and Fracture Mechanics of Engineering Materials*. New York: John Wiley and Sons.
- Inglis, C.E. (1913). Stresses in plate due to the presence of cracks and sharp corners. *Transaction of the Institution of Naval Architects*, 55(41), 219.
- Kilian, H.G., Enderle, H.F. and Unseld, K. (1986). The use of the van der Waals model to elucidate universal aspects of structure property relationships in simply extended dry and swollen rubbers. *Colloid and Polymer Science*, 264, 866-876.
- Kim, W.D., Lee, H.J., Kim, J.Y. and Koh, S.K. (2004). Fatigue life estimation of an engine rubber mount. *International Journal of Fatigue*, 26, 553-560.
- Lee, Y.L., Pan, J., Hathaway, R.B. and Barkey, M.E. (2005). *Fatigue Testing and Analysis. Theory and Practice*. Elsevier Inc.
- Lira, W.L., Cavalcanti, P.R., Coelho, L.C.G. and Martha, L.F. (2002). A modelling methodology for finite element mesh generation of multi-region models with parameter surfaces. *Journal of Computational and Graphical Statistics*, 6, 907-918.
- Liu, Y. and Mahadevan, S. (2005). Multiaxial high-cycle fatigue criterion and life prediction for metals. *International Journal of Fatigue*, 27, 790-800.

- Makkonen, M. (2009). Predicting the total fatigue life in metals. *International Journal of Fatigue*, 31, 1163-1175.
- Marcus, M., Frank, S. and Carsten, M.W. (n.d). *Creation of Finite Element Models of Human Body Based Upon Tissue Classified Voxel Representations*. Germany: University of Karlsruhe.
- Mars, W. V., Mars and Fatemi, A. (2002). A literature survey on fatigue analysis approaches for rubber. *International Journal of Fatigue*, 24, 949-961.
- Ogden, R. W. (1984). *Non-linear Elastic Deformation*. Ellis Horwood Limited.
- Osman, M.H. (2004). *Finite Element Modeling of Sheet Metal Bending*, 2, 34-36.
- Papadopoulos, I.V., Davoli, P., Gorla, C., Filippini, M. and Bernasconi, A. (1997). A comparative study of multiaxial high-cycle fatigue criteria for metals. *International Journal of Fatigue*, 19, 219-235.
- Philip, A.S. (2006). *Corrosion of Polymers and Elastomers* (2<sup>nd</sup> edn.). CRC Press.
- Rivlin, R.S. and Thomas, A.G. (1953). Rupture of rubber. I. Characteristic energy for tearing. *Journal of Polymer Science*, 10, 291-318.
- Saintier, N., Cailletaud, G. and Piques, R. (2006). Crack initiation and propagation under multiaxial fatigue in a natural rubber. *International Journal of Fatigue*, 28, 61-72.
- Saintier, N., Cailletaud, G. and Piques, R. (2006). Multiaxial fatigue life prediction for a natural rubber. *International Journal of Fatigue*, 28, 530-539.
- Wang, B., Lu, H. and Kim, G. A. (2002). Damage model for the fatigue life of elastomeric materials. *Mechanics of Materials*, 34, 475-483.
- Weber, G. and Anand, L. (1990). Finite deformation constitutive equations and a time integration procedure for isotropic, hyperelastic-viscoplastic solids. *Computer Methods in Applied Mechanics and Engineering*, 79, 173-202.
- Wöhler, A. (1867). Wöhler experiments on the strength of metals. *Engineering* 2(1867), 160.
- Yeoh, O.H. (1993). Some forms of the strain energy function for rubber. *Rubber Chemistry and Technology*, 66, 754-771.